Egypt. J. Soil Sci. **Vol. 63**, No. 4, pp: 581-691 (2023)

Egyptian Journal of Soil Science

http://ejss.journals.ekb.eg/

Assessment and Development of Pedotransfer Functions to Estimate Soil Saturated Hydraulic Conductivity in Arid Soils with Application to GIS Mapping in the Al-Ahsa Oasis, Saudi Arabia

Abdullah Hassan Al-Saeedi

Department of Environmental and Natural Resources, College of Agricultural and Food Sciences, King Faisal University, P. O. Box 420, Al-Hassa 31982, Saudi Arabia

AL-AHSA is one of the oldest and largest agricultural regions in Saudi Arabia. It was determined that thirty soil samples representing the majority of soil types within the region were collected and analyzed for their physical and hydraulic properties in a laboratory, including particle size (sand percent, silt percent, clay percent), saturation percent (θs), bulk density (ρ), calcium carbonate percent ($CaCO_3$), Field capacity (FC), wilting point (WP), and saturated hydraulic conductivity (Ks). A comprehensive statistical analysis was conducted to develop a pedotransfer function (PTF) to predict potential relationships between physical properties and Ks values based on correlation, stepwise multiple linear regression, mean square error (MSE), root mean square error (RMSE), t-test, and Nash-Sutcliffe efficiency (NSE). In a stepwise analysis, both sand and ρ highly influence the outcome. A significant correlation was found with Ks equal to (0.755), MSE equal to 0.045, RMSE equal to 0.194, and satisfactory NSE equal to 0.581. Using the spatial interpolation technique of the GIS map program, a new model was applied to more than 500 points of soil data in order to develop a new spatial pattern map based on the Ks value. The map is designed to provide an easy-to-read and quick-reach guide for environmental researchers and engineers in determining the Ks value in the studied area in Al-Ahsa Oasis.

Keywords: Al-Ahsa; Pedotransfer; Soil hydraulic; Soil mapping, GIS.

1. Introduction

Soil-saturated hydraulic conductivity (Ks) is essential in all aspects of geotechnical engineering, environmental management, water resource management, hydrological models, and soil moisture balance. Models of water and solute dynamics attribute significant importance to saturated hydraulic conductivity (Ks), which explains its recognition as an input parameter (Perera et al., 2005; Rafie & El-Boraie, 2017; Zapata et al., 2000). Nonetheless, Ks exhibits heterogeneous spatial and temporal patterns as well as scale dependency (Santra et al., 2018; Sobieraj et al., 2004). A different result can be obtained for Ks in the same area, as well as for the same sample size, depending on the measurement method and scale (Braud et al., 2017). For an accurate characterization of the spatial variability of Ks in a study area, it is generally necessary to collect large numbers of soil samples. The measurement of Ks directly is strenuous, rottenly labor-intensive, time-consuming, and expensive (Li et al. 2007; Zhang et al. 2019). A pedotransfer function (PTF) has been developed to overcome these limitations and the lack of measured data so that estimates of Ks for large regions can be obtained. Increasingly, soil surveys and existing soil databases provide an alternative to measuring soil properties indirectly, such as Ks (Al-Saeedi, 2022a; Pachepsky et al., 2015; Tomasella & Pachepsky, 2003). Over the past four decades, the PTF models have prospered as hydrological and environmental models have flourished. Through long-term research, two types of

*Corresponding author e-mail: aalsaeedi@kfu.edu.sa
Received: 05/08/2023; Accepted: 27/08/2023
DOI: 10.21608/EJSS.2023.227275.1631

PTF were distinguished in terms of input data, namely, class pedotransfer functions were utilized to determine the average hydraulic characteristics of soil texture classes distinct from one another. A continuous pedotransfer function was used to determine soil hydraulic characteristics based on measures of sand particle size, bulk density, and clay, silt, and organic matter percentages (Wösten et al., 1995). On the other hand, many mathematical models have been developed, including regression trees (Pachepsky et al., 2015), artificial neural networks (Schaap et al., 1998; Trejo-Alonso et al., 2021; Y. Zhang & Schaap, 2019), group methods of data handling (Ungaro et al., 2005), and support vector machines (Twarakavi et al., 2009). Regardless of the number of samples and data used, the accuracy of the generated PTF is likely to result in poor estimation accuracy when applied to soils that are different from the soils from which it was generated (Bilardi et al., 2020; Vereecken et al., 1992; Weynants et al., 2009). As a result, it is highly recommended to develop PTFs from local data rather than from data developed outside the local domain (Kotlar et al., 2019; Omran et al., 2022; Tomasella et al., 2000; Vereecken et al., 1992) . The percentage of sand and clay in the soil and the bulk density showed a good correlation with the laboratory-measured Ks in medium-textured soils when compared to other physical and hydraulic properties (Borek et al., 2021; Saxton et al., 1986; Y. Zhang & Schaap, 2019; Zhao et al., 2016). Abdelbaki (2021) performed a comprehensive evaluation of 45 PTFs, which are described as the best performing PTFs. The PTFs were divided into four groups based on the input requirements they required. These forty-five PTFs showed poor performance, for both as total soils and when grouped according to texture. In arid climate regions where less precipitation and high soil evaporation, which led to rare vegetation blanket, soil characterized by almost no organic content with the domination of sand fraction and high content of gypsum and calcium carbonates $CaCO_3$ (Bahnasawy, 2017; Francis & Aguilar, 1995). Calcium carbonate is commonly precipitated as the size of silt fraction or bonds to clay and/or silt particles behave like coarse sand (Al-Saeedi, 2022b; Fairbridge and Finkl, 1979). Moreover, calcareous soils contain a high amount of calcium carbonate in the form of micritic or microsparitic crystals. These crystals can develop within soils and precipitate gradually in clayey or silt micromasses, thereby filling the pores between soil particles and aggregates over time (Durand et al., 2010). Consequently, the soil's hydraulic conductivity can be severely reduced due to the reduction in the size and number of pores (Karim & Fattah, 2020).

Al-Ahsa is an agricultural settlement that is among the oldest and largest in the region. As of recently, date palms have become the dominant crop tree, with more than three million trees (Al-Wusaibai et al., 2012). The soil of Al-Ahsa consists primarily of sand and sandy loam, with very little clay and organic carbon present in the cultivated area (Al-Barrak & Al-Badawi, 1988); $CaCO_3$ levels are high (Bashour et al., 1983), aggregated in the form of sand and silt particles (Al-Hawas, 1989). Therefore, the aim of this study was designed to provide an easy-to-read and quick-reach guide for environmental researchers and engineers in determining the Ks value in the studied area in Al-Ahsa Oasis.

2. Material and methods

2.1 Soil sampling and testing

Thirty-six samples were collected from different locations throughout the Al-Ahsa region. Samples were air-dried and crashed to pass through 2 mm sieves. Saturated hydraulic conductivity Ks was measured using a PVC (Polyvinyl chloride) cylinder with 5 cm diameter and 20 cm height. A perforated screen was fitted to the base of the cylinder, and filter paper was placed between the soil and the screen to prevent the migration of fine particles during the test. A disturbed sample of each soil was poured into the cylinder and compacted equally to the bulk density ρ. Another filter paper was also placed over the soil surface to minimize soil disturbance before exerting a constant head of about 15cm. The assembly was held in a vertical position using a panel frame. The soil columns were set in duplicate in the laboratory at a room temperature of 25 ±5 Co. After reaching the soil columns to saturated state, the data of effluent water was recorded for each sample for a period of one hour. Having measured the water discharge. Using Darcy's law, which takes the following form, was applied to determine the Ks of each soil eq.1:

$$Ks = \frac{Q\Delta L}{A\Delta H} \quad (1)$$

Ks is saturated hydraulic conductivity (cm min-1), ΔL is the soil column length (cm), A is the cross-sectional area (cm2), and ΔH is the difference in hydraulic head across the column ends (cm) (Reynolds et al., 2002). Acid neutralization method was used for determining calcium carbonate (CaCO3) contents as described in Rowell, (1994). Soil particle size, bulk density ρ, and saturation percentage θs were measure in the laboratory according to the standard methods of SSSA (Soil

Science Society of America) (Reynolds et al., 2002). Moisture at field capacity FC (-33 kPa) and Wilting point (-1500 kPa) were extracted from soil water characteristics curve (SWCC) using filter paper methods (Al-Khafaf & Hanks, 1974; Al-Saeedi, 2022b; Bulut & Leong, 2008). A descriptive statistical summary of the soil data is shown in Table 1,

Table 1. Descriptive statistics of the saturated hydraulic conductivity Ks, $CaCO_3$, percentage of soil size class (*Sand, Silt, and Clay*), bulk density (ρ), saturation (θ_s), field capacity (FC), and wilting point (WP).

Variable	Obs. No.	Minimum	Maximum	Mean	SD
Sand %	30	12.000	95.380	47.078	23.804
Silt %	30	1.610	86.000	47.854	24.607
Clay %	30	1.000	19.000	5.068	4.590
$CaCO_3$%	30	1.250	71.233	30.069	22.642
ρ ($g.cm^{-3}$)	30	0.960	1.550	1.233	0.197
θ_s ($cm^3.cm^{-3}$)	30	0.233	0.566	0.410	0.093
FC ($cm^3.cm^{-3}$)	30	0.031	0.366	0.210	0.082
WP ($cm^3.cm^{-3}$)	30	0.024	0.206	0.121	0.044
Ks ($cm.min^{-1}$)	30	0.004	1.000	0.227	0.333

SD: Standard deviation

2.2 Statistical analysis

Two types of analysis were performed. Firstly, identify the relationship between the data. Secondly, using these relations to establish a potential estimation equation for Ks. The correlation coefficient using equation (2) was tested between all hydraulic properties and parameters.

$$R = \frac{\sum(x_i-\bar{x})(y_i-\bar{y})}{\sqrt{\sum(x_i-\bar{x})^2\sum(y_i-\bar{y})^2}} \quad (2)$$

The x_i and y_i are measured and estimated variables, respectively, $\bar{x}$ and $\bar{y}$ are the mean.

A stepwise regression equation (limited for tow variables maximum) was used to estimate the Ks using equation (3).

$$y_i = \beta_0 + \beta_{i1}x_1 + \beta_2 x_{i2} + \cdots + \beta_n x_{in} \quad (3)$$

β is the slope.

Lowest mean square error (MSE) equation (4) was used to select the best equation among tested properties.

$$MSE = \frac{1}{n}\sum_{i=1}^{n}(y_i - \bar{y_i})^2 \quad (4)$$

Root mean square (RMSE) is a common metric used to determine the variance between predicted and measured values. The ideal model should have a minimum RMSE value that is positive in comparison with other models (Schaap, 2004).

$$\text{RMSE} = \sqrt{\sum_{i=1}^{n}\frac{(x_i-y_i)^2}{n}} \quad (5)$$

Among the most appropriate objective functions to provide reliable information about the overall goodness of fit of a model is the NSE (Nash–Sutcliffe efficiency) (Legates & Mccabe, 1999; McCuen et al., 2006; Nash & Sutcliffe, 1970). The Nash-Sutcliffe efficiency (NSE) is a statistic indicating the relative magnitude of residual variance ("noise") with respect to the predicted data variance (Moriasi et al., 2007). An NSE is described by Nash and Sutcliffe (1970) as a measure of the compliance between a predicted data plot and the measured data plot, with a coefficient of efficiency that ranges from minus infinity to one (0.01 to 1.0), with higher values indicating a higher degree of agreement. A value of zero indicates that the observed mean is as good a predictor as the model, and a negative value indicates that the observed mean is a more reliable predictor than the model (Wilcox et al., 1990). The literature indicates that NSE values can be classified into four general categories: less than 0.5 is considered unsatisfactory, 0.50 - 0.70 is considered satisfactory, 0.70 - 0.80 is considered good, and > 0.80 is considered very good (Moriasi et al., 2015). The form of NSE equation:

$$\text{NSE} = 1 - \frac{\sum_{i=1}^{n}(\bar{y}_i-y_i)^2}{\sum_{i=1}^{n}(\bar{y}_i-Y)^2} \quad (6)$$

2.3 PTFs selection

This study selected the best performed PTFs for the non-grouped texture dataset (2 equations) (Abdelbaki, 2021), namely, Cosby et al., (1984) equation 7 and Ottoni et al., (2019) equation 8.

$$Ks(cm/min) = 0.0423 \times 10^{(-0.6+0.0126\times Sand\%-0.0064\times clay\%)} \quad (7)$$

$$Ks(cm/min) = \frac{10^{(3.998-0.0101\times Silt\%-0.0152\times Clay\%-1.163\times \rho}}{1440} \quad (8)$$

The performance of these PTFs (eq.7 and 8) will be statistically compared with the new PTF that is generated through stepwise regression using the minimum inputs of accessible local soil data.

2.4 Mapping Ks and GIS Interpolation Method

Soil data were provided by Elprince et al. (2003). Five hundred and sixty-six grid nods (380 m by 500 m) were used to collect one composite sample, which included samples from 0 to 20 cm depth. The samples were ground into element gravels after they had been air-dried, ground, thoroughly mixed, and passed through a 2 mm sieve. According to the standard hydrometer method, soil texture (percentage of sand, silt, and clay) was determined (Gee & Bauder, 1986). Soil bulk density was determined using the Al-Saeedi, (2022b) well-tested local statistical equation.

Geographic information systems (GIS) are computerized systems that contain rules and procedures for analyzing and processing geographical data. These algorithms are designed to link geographical data to their coordinates and to group data into layers based on their locations and display the data on a map to illustrate the geographical characteristics of an area. The spatial and geotechnical data for each sample point are arranged and tabulated in an Excel sheet in a manner compatible with ArcMap 10.4.

In general, interpolation refers to the estimation of a value based on the relation between two known values in a sequence of values, i.e., a method of predicting grid values in specific locations where samples are not readily available (Childs, 2004). Due to the high density of data in the study area, inverse distance weighting (IDW) is the most appropriate method for interpolating dense data (Childs, 2004). Using IDW, values are estimated at unmeasured points by combining values at nearby measured points (Longley & Frank Goodchild, 2020). Interpolation in two dimensions can be performed based on parameter measurements at non-scaled locations z_i to determine the parameter z in non-scaled locations. The parameter can be used to represent any property of soil. Based on the equation, the IDW algorithm is used:

$$Z_i = \frac{\sum_{i=1}^{N} Z_i . d_i^{-n}}{\sum_{i=1}^{N} d_i^{-n}} \quad (9)$$

Using Z_0 as the estimation value of the variable z in point i, z_i as the sample value, d_i as the distance between the sample point and the estimated point, N as the coefficient determining weight based on distance, and n as the total number of predictions for each validation case.

3. Results

3.1 Soil properties statistics

As shown in Figure 1, the samples in this study include sandy loam (SL), loam (L), sandy (S), silty loam (SiL), and loamy sand (LS). The sand% ranged from 12% to 95.380%, with a mean of 47.078% and a standard deviation of 23.804%. With a maximum value of 86.000% and a low value of 1.610 %, silt was closer to sand with a mean of 47.854 and a standard deviation of 24.607. Clay is low in most samples, with a mean of 5.068%, three samples above 10%, a maximum value of 19.000%, and a minimum value of 1.000% with a standard deviation of 4.590%. Several studies have reported that sand dominates other soil elements in arid and semi-arid regions (Al-Barrak & Al-Badawi, 1988; Al-Hawas et al., 2020; Al-Sayari & Zötl, 1978; Francis & Aguilar, 1995).

The $CaCO_3$ percentage ranged from 1.250% to 71.233%, with a mean of 30.069% and a standard deviation of 22.642%. As a constituent element in Al-Ahsa soils, calcite $CaCO_3$% is either formed directly from the parent material or precipitated by direct irrigation water or water rising through capillarity (Elprince, 1985). Table 2 illustrates that $CaCO_3$ percentage was highly positively correlated with silt percentage, which implies the size of $CaCO_3$ particles was reflected in the size of silt particles. This finding is consistent with other studies in arid regions.

(AlJaloud, 1983; Chaudhari et al., 2013; Chen et al., 2020; Hafshejani & Jafari, 2017).

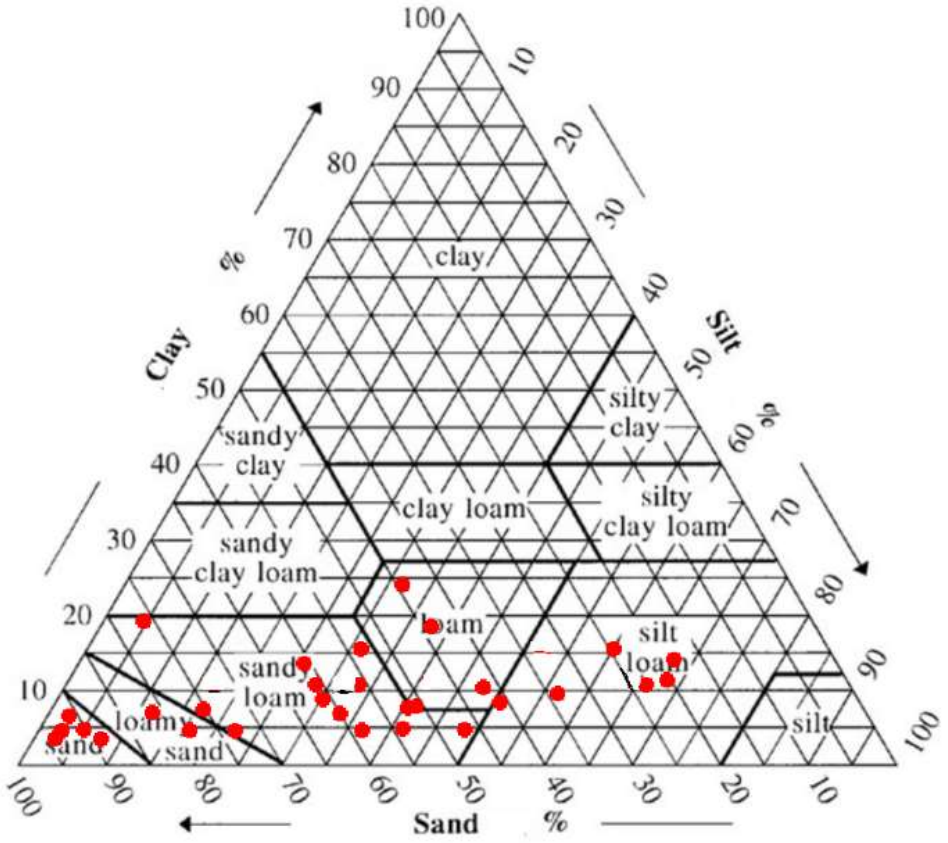

Fig. 1. Texture classes of the soil samples of Al-Ahsa (clay (≤2 µm), silt (2–50µm), sand (50–2000 µm)] according to USDA classification.

The bulk density ranged between 0.960 g.cm^{-3} and 1.550 g.cm^{-3} with a mean of 1.233 g.cm-3 and a standard deviation of 0.197 g.cm-3 (Table 1). The value of ρ increased as the percentage of sand increased, whereas the value decreased as the percentage of $CaCO_3$%, silt%, and clay% increased. This is known as the increase of $CaCO_3$% in soil, which is well documented to have a low density as reported by (Chaudhari et al., 2013; Chen et al., 2020)

The soil saturation coefficients ranged from 0.233 to 0.566, with a mean of 0.410 and a standard deviation of 0.093%. As shown in Table 2, saturation (θs) was negatively correlated with sand percentage and ρ with R values of -0.800 and -0.903, respectively. Unlike silt and CaCO3 percentages have a high positive correlation of 0.806 and 0.753, respectively. The results agree with the benefits of both the pore ratio and the fine particles (Chaudhari et al., 2013; Du, 2020; Saxton et al., 1986; Sun et al., 2020).

It was found that the field capacity FC and wilting point WP ranged from 0.031 and 0.024 cm3 cm-3 to 0.366 and 0.206 cm3 cm-3, with a mean of 0.210 and 0.121 cm3 cm-3, and SD of 0.082 and 0.044 cm3 cm-3, respectively (Table 1). Both parameters were positively correlated with $CaCO_3$, Silt, and θs. Conversely, a negative result is a Sand and ρ (Table 2). As a result of this study, soils for which sand and $CaCO_3$ dominant soil is showing that ρ has more influence over clay percentage for moisture content under high soil potential than sand and $CaCO_3$. An earlier study supporting this finding examined the effect of pores ratio and density on a wide range of soil potentials. (Gao & Sun, 2017; Ostovari et al., 2015; Shiri et al., 2017).

According to Table 1, saturated hydraulic conductivity Ks ranged from 0.004 to 1.000 cm.min^{-1} with a mean of 0.227 cm.min^{-1} and a standard deviation of 0.333 cm.min^{-1}. As Ks showed no correlation with Clay, FC, and WP, however, Sand and Silt exhibited a high correlation of 0.630 and 0.588 respectively and a fairly weak correlation with $CaCO_3$, θs, and ρ with values of (-0.397), (-0.325), and 0.316 respectively. In sandy-dominated soils the

macro pores have more effect than micropores on determining the value of Ks (Abdelbaki, 2021; Dabral and Pandey, 2016; Shwetha and Prasanna, 2018).

3.2 PTF development and assessment

Using a comprehensive stepwise regression analysis using the Lowest Mean Square Error (MSE) as a criterion factor with only two variables were retained in this model. Table 3 shown the standard error and t value significancy of the tested parameters, only Sand% and ρ showed significant effect on the prediction value of Ks. Equation 10 consequently was generated from the stepwise analysis , with a high significant correlation of 0.755 and low MSE 0.045.

Table 2. The Matrix correlation coefficient between soil physical properties sand%, silt%, clay%, and bulk density (ρ), saturation (θs), field capacity (FC), and wilting point (WP), and saturation conductivity (Ks).

	$CaCO_3$, %	Sand, %	Silt, %	Clay, %	ρ ($g.cm^{-3}$)	θ_s ($cm^3.cm^{-3}$)	FC ($cm^3.cm^{-3}$)	WP ($cm^3.cm^{-3}$)
Sand %	-0.826***							
Silt %	0.843***	-0.982***						
Clay %	-0.238ns	0.081ns	-0.265ns					
ρ ($g.cm^{-3}$)	-0.812***	0.849***	-0.864***	0.228ns				
θ_s ($cm^3.cm^{-3}$)	0.753***	-0.800***	0.806***	-0.173ns	-0.902***			
FC ($cm^3.cm^{-3}$)	0.554***	-0.550***	0.558***	-0.138ns	-0.658***	0.665***		
WP ($cm^3.cm^{-3}$)	0.440**	-0.450**	0.437**	-0.014ns	-0.582***	0.606***	0.904***	
Ks ($cm.min^{-1}$)	-0.397**	0.630***	-0.588***	-0.114ns	0.316*	-0.325*	-0.165ns	-0.143ns

* Significant at p< 0.1; ** significant at p< 0.05; *** significant at p< 0.01 levels of probability, ns not significant

Table 3. Saturated conductivity (Ks) stepwise regression analysis for soil variables significancy using *t*-test results. Correlation coefficient (R) and mean standard error (MSE).

Variable	St. Error	*t*	Pr > |t|
Sand, %	0.003	5.433	**<0.0001**
Silt, %	0.000		
Clay, %	0.000		
$CaCO_3$, %	0.000		
ρ ($g.cm^{-3}$)	0.405	-3.292	**0.003**
θ_s ($cm^3.cm^{-3}$)	0.000		
FC ($cm^3.cm^{-3}$)	0.000		
WP ($cm^3.cm^{-3}$)	0.000		
R	0.755^{***}		
MSE	0.045		

*** Significant at p< 0.001 levels of probability

$$Ks(cm/min) = |1.015 + 0.018 * Sand\% - 1.333 * \rho| \quad (10)$$

(Absolute value was used to avoid any negative values for Ks particularly in the fine side soils).

According to Table 4, the correlation values for the three used models were high and significant, and the RMSE for model 10 is lower than that for models 7 and 8, with 41% and 42% respectively. Both models 7 and 8 had negative NSE values, indicating that they were invalid for estimating Ks (Moriasi et al., 2015;

Wilcox et al., 1990). A satisfactory result was obtained for model 10 with R equal to 0.766, MRSE equal to 0.193, and NSE equal to 0.581. There is a strong correlation between coarse particles and large pores in sandy soils, which contributes significantly to the structure of the suggested models. This is in conjunction with numerous studies that attempted to estimate Ks based on soil physical parameters. (Abdelbaki, 2021; Shwetha and Prasanna, 2018).

3.3 Mapping Ks

Figure 2 shows the spatial pattern of saturation conductivity Ks. High values of Ks ranged between 0.44-0.68 cm min^{-1} were depicted in Figure 2 in the northeast side of the oasis. Most of the rest area Ks ranged between 0.025 and 0.0081cm min^{-1}. The lowest Ks values were in the northwest with a range of 0.0081 to 0,16 cm min^{-1}.

Table 4. Statistical evaluation of the used models, correlation coefficient (R), root mean square error (RMSE), and Nash–Sutcliffe efficiency (NSE).

	Eq. 7	Eq. 8	Eq. 10
R	0.690***	0.748***	0.766***
RMSE	0.320	0.331	0.194
NSE	-0.148	-0.227	0.581

*** significant at p< 0.01 levels of probability

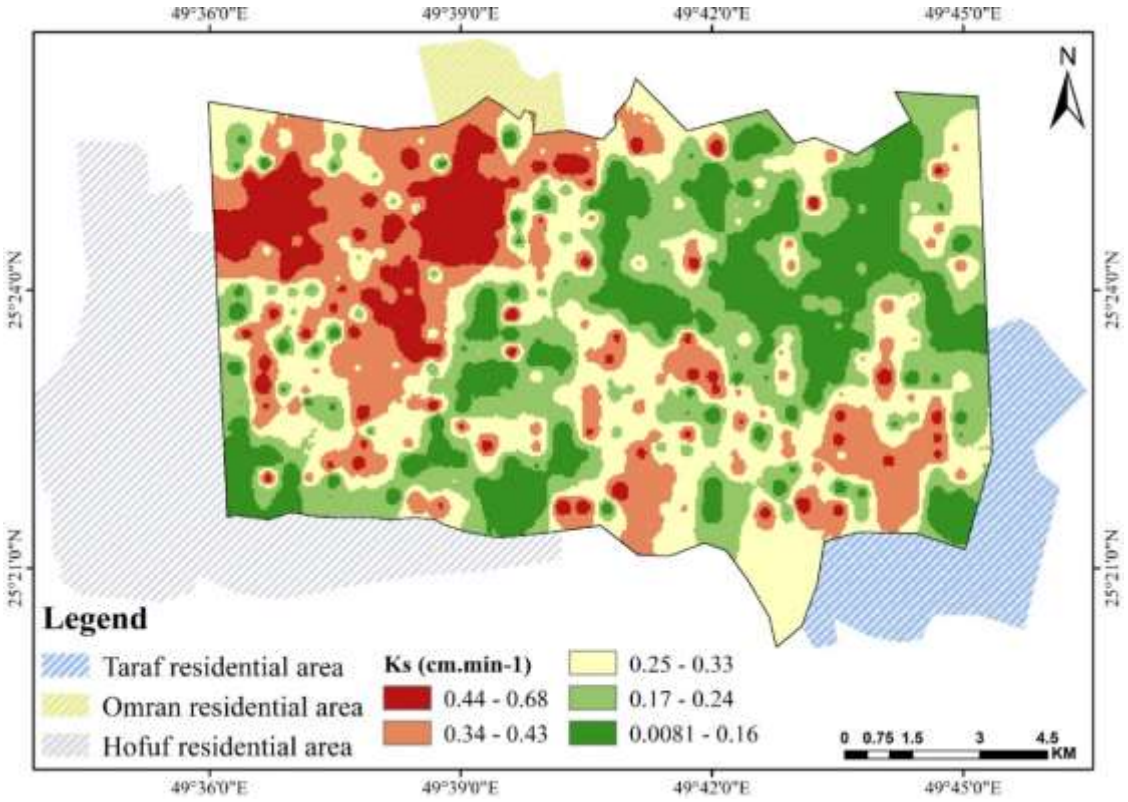

Fig. 2. Spatial pattern of saturated conductivity (Ks) over the study area in Al-Ahsa.

4. Discussion

Sand dominates other soil elements in arid and semi-arid regions in general and in Al-Ahsa in particularly as reported by several studies (Al-Barrak & Al-Badawi, 1988; Al-Hawas et al., 2020; Al-Sayari & Zötl, 1978; Francis & Aguilar, 1995).

As a constituent element in Al-Ahsa soils, calcite $CaCO_3$% is either formed directly from the parent material or precipitated by direct irrigation water or

water rising through capillarity (Elprince, 1985). which implies the size of $CaCO_3$ particles was reflected in the size of silt particles more than clay particales. This finding is consistent with other studies in arid regions (AlJaloud, 1983; Chaudhari et al., 2013; Chen et al., 2020; Hafshejani & Jafari, 2017).

The value of ρ increased as the percentage of sand increased, whereas the value decreased as the percentage of $CaCO_3$%, silt%, and clay% increased. This is known as the increase of $CaCO_3$% in soil, which is well documented to have a low density as reported by (Chaudhari et al., 2013; Chen et al., 2020).

The results of θs agreed with the benefits of both the $CaCO_3$ and silt percentage in the high calcareous soil this effect as already shown on ρ values, this finding supported by many researches (Chaudhari et al., 2013; Du, 2020; Saxton et al., 1986; Sun et al., 2020).

As a result of this study, soils whereas sand is a dominant the ρ shows more influence than clay percentage in determining the moisture content under soil potential. An earlier study supporting this finding examined the effect of pores ratio and density on a wide range of soil potentials. (Gao & Sun, 2017; Ostovari et al., 2015; Shiri et al., 2017).

Ks value in sand-dominated soils, as Al-Ahsa, for sensitive for the losing structure and macro pores, which were resulted from the high percentage of sand percentage, even with the existing of $CaCO_3$ to the micropores (Abdelbaki, 2021; Dabral and Pandey, 2016; Shwetha and Prasanna, 2018).

The stepwise regression analysis showed a strong correlation between coarse particles and large pores in sandy soils, which contributes significantly to the structure of the suggested models, this was reflected in the value of correlation and the significancy of *t* values for both sand percentage and ρ in the stepwise multi regression test. Equation 10 was generated based on this result. This is in conjunction with numerous studies that attempted to estimate Ks based on soil physical parameters. (Abdelbaki, 2021; Shwetha and Prasanna, 2018).

Model 10 showed a better estimation result with RMSE lower than that for models 7 and 8, with 41% and 42% respectively. The negative values of NSE in model 7 and 8 indicating that they were invalid for estimating Ks (Moriasi et al., 2015; Wilcox et al., 1990). A satisfactory result was obtained for model 10 with R equal to 0.766, MRSE equal to 0.193, and NSE equal to 0.581.

The general Pattern of Ks map was highly affected by the high content of sandy soil (Al-Saeedi, 2022c). The decrease in Ks occurred as the land depressed toward the east toward increasing silt percentage and $CaCO_3$ content values, as reported earlier in (Al-Saeedi, 2022c), this resulting in a reduction in the value from 0.16 cm. min^{-1} to 0.0081 cm. min^{-1} . In general, the value of Ks is relatively high due to the high sand content (AlJaloud, 1983).

5. Conclusion

Sand dominates the soil particle size inAl-Ahsa, while clay is scarce, which affects the distribution of macropores that control the flow of water in the saturation state (Ks). To improve the performance and accuracy of any given model, more and more detailed research must be conducted to include a greater number of samples. A GIS-based digital map allows field researchers and planners to study any location quickly and accurately.

5. Conflict of Interest

The author declares that he has no known competing financial interests or personal relationships that could have appeared to influence the work reported in this paper.

6. Acknowledgement

Author would like to thank Dr. Abdulhalim Hassaballah for his assistant in GIS program.

7. References:

Abdelbaki, A. M. (2021). Selecting the most suitable pedotransfer functions for estimating saturated hydraulic conductivity according to the available soil inputs. Ain Shams Engineering Journal, 12(3),2603–2615. https://doi.org/10.1016/j.asej.2021.01.030

Al-Barrak, S. A., & Al-Badawi, M. (1988). Properties of some salt affected soil in Al-Hassa, Saudi Arabia. Arid Soil Research and Rehabilitation , 2, 85–95.

Al-Hawas, I. A. (1998). Origin and properties of some phyllosilicate minerals in the soils of the Al-Hassa oasis, Saudi Arabia. PhD Thesis, Department of Soil Science, University of Reading, Reading.

Al-Hawas, I. A., Hassan, S. A., & Abdeldayem, H. M. (2020). Potential applications in relation to the various physicochemical characteristics ofAl-Ahsa oasis clays in Saudi Arabia. Applied Sciences (Switzerland), 10(24), 1–22. https://doi.org/10.3390/app10249016

AlJaloud, A. A. (1983). Effect of reclamation on Al-Hassa saline soil in Saudi Arabia [Master]. Master's Thesis, Department of Agriculture and Home Economics, California State University, Los Angels, CA, USA.

Al-Khafaf, S., & Hanks, R. J. (1974). Evaluation of the filter paper method for estimating soil water potential. Soil Science, 117(4). https://doi.org/10.1097/00010694-197404000-00003.

Al-Saeedi, A. H. (2022a). Assessment of different pedotransfer models using soil texture for predicting saturated water content, Al-Ahsa, Saudi Arabia.

Al-Saeedi, A. H. (2022b). Characterizing physical and hydraulic properties of soils in Al-Ahsa, Kingdom of Saudi Arabia. Saudi Journal of Biological Sciences, 29(5), 3390–3402. https://doi.org/10.1016/j.sjbs.2022.01.061.

Al-Saeedi, A. H. (2022c). Using a pedotransfer (PTF) model to establish GIS-based maps for the main physical and hydraulic soil properties in the eastern region of the Al-Ahsa Oasis, Saudi Arabia. PLOS ONE, 17(10), e0276259. https://doi.org/10.1371/journal.pone.0276259.

Al-Sayari, S. S., & Zötl, J. G. (1978). Quaternary Period in Saudi Arabia. In S. S. Al-Sayari & J. G. Zötl (Eds.), Quaternary Period in Saudi Arabia. Springer Vienna. https://doi.org/10.1007/978-3-7091-8494-3

Al-Wusaibai, N. A., ben Abdallah, A., Al-Husainai, M. S., Al-Salman, H., & Elballaj, M. (2012). A comparative study between mechanical and manual pollination in two premier Saudi Arabian date palm cultivars. Indian Journal of Science and Technology, 5(4), 2487–2490. https://doi.org/10.17485/ijst/2012/v5i4.4.

Bahnasawy, N. (2017). Sand Mineralogy As a Criterion for Soil Uniformity North West Wadi El-Natrun. Egyptian Journal of Soil Science, 56(4), 739–759. https://doi.org/10.21608/ejss.2017.1522.

Bashour, I. I., Al-Mashhady, A. S., Devi Prasad, J., Miller, T., & Mazroa, M. (1983). Morphology and composition of some soils under cultivation in Saudi Arabia. Geoderma, 29(4), 327–340. https://doi.org/10.1016/0016-7061(83)90019-8

Bilardi, S., Ielo, D., & Moraci, N. (2020). Predicting the Saturated Hydraulic Conductivity of Clayey Soils and Clayey or Silty Sands. Geosciences, 10(10), 393. https://doi.org/10.3390/geosciences10100393

Borek, Ł., Bogdał, A., & Kowalik, T. (2021). Use of pedotransfer functions in the rosetta model to determine saturated hydraulic conductivity (Ks) of arable soils: A case study. Land, 10(9). https://doi.org/10.3390/land10090959

Braud, I., Desprats, J. F., Ayral, P. A., Bouvier, C., & Vandervaere, J. P. (2017). Mapping topsoil field-saturated hydraulic conductivity from point measurements using different methods. Journal of Hydrology and Hydromechanics, 65(3), 264–275. https://doi.org/10.1515/johh-2017-0017

Bulut, R., & Leong, E. C. (2008). Indirect measurement of suction. Geotechnical and Geological Engineering, 26(6), 633–644. https://doi.org/10.1007/s10706-008-9197-0

Chaudhari, P. R., Ahire, D. V, Ahire, V. D., Chkravarty, M., & Maity, S. (2013). Soil Bulk Density as related to Soil Texture, Organic Matter Content and available total Nutrients of Coimbatore Soil. International Journal of Scientific and Research Publications, 3(1), 2250–3153. www.ijsrp.org

Chen, L., Chen, X., Yang, X., Bi, P., Ding, X., Huang, X., & Wang, H. (2020). Effect of Calcium Carbonate on the Mechanical Properties and Microstructure of Red Clay. Advances in Materials Science and Engineering, 2020. https://doi.org/10.1155/2020/5298186.

Childs, C. (2004). Interpolating Surfaces in ArcGIS Spatial Analyts. ArcUser, 3235(July-September), 32–35. papers2://publication/uuid/7A4DAFEA-CE6C-44AE-9DC4-AE9B953BB87A

Cosby, B. J., Hornberger, G. M., Clapp, R. B., & Ginn, T. R. (1984). A Statistical Exploration of the Relationships of Soil Moisture Characteristics to the Physical Properties of Soils. Water Resources Research, 20(6), 682–690. https://doi.org/10.1029/WR020i006p00682

Dabral, P. P., & Pandey, P. K. (2016). Models to estimate soil moisture retention limits and saturated hydraulic conductivity. Journal of Indian Water Resources Society, 36(1), 50–55.

Du, C. (2020). Comparison of the performance of 22 models describing soil water retention curves from saturation to oven dryness. Vadose Zone Journal, 19(1). https://doi.org/10.1002/vzj2.20072

Durand, N., Monger, C. H., & Canti, M. G. (2010). Calcium Carbonate Features. In Interpretation of Micromorphological Features of Soils and Regoliths (Issue December, pp. 149–194). Elsevier B.V. https://doi.org/10.1016/B978-0-444-53156-8.00009-X

Elprince, A. M. (1985). Model for the Soil Solution Composition of an Oasis. Soil Science Society of America Journal, 49(5), 1121–1128. https://doi.org/10.2136/sssaj1985.03615995004900050010x.

Elprince, A. M., Al-Dakheel, Y., Al-Saeedi, A. H., Hussein, A., & Massoud, M. A. (2003). National Fertilizer Program for Date Palm: Al-Hassa Phase-Final Report (FRQ704).

Fairbridge, R. W., & Finkl, C. W. (1979). Encyclopedia of Soil Science: Part I, Physics, Chemistry, Biology, Fertility and Technology. Van Nostrand Reinhold.

Francis, R. E., & Aguilar, R. (1995). Calcium carbonate effects on soil textural class in semiarid wildland soils. Arid Soil Research and Rehabilitation, 9(2), 155–165. https://doi.org/10.1080/15324989509385882

Gao, Y., & Sun, D. (2017). Computers and Geotechnics Soil-water retention behavior of compacted soil with different densities over a wide suction range and its prediction. Computers and Geotechnics, 91, 17–26. https://doi.org/10.1016/j.compgeo.2017.06.016

Gee, G. W., & Bauder, J. W. (1986). Particle Size Analysis. In A. Klute (Ed.), Methods of Soil Analysis, Part 1 (2nd ed., pp. 383–411). Soil Science Society of America: Madison, WI, Agron. 9.

Hafshejani, N. A., & Jafari, S. (2017). The study of particle size distribution of calcium carbonate and its effects on some soil properties in khuzestan province. Iran Agricultural Research, 36 (2)(2), 71–80.

Karim, T. H., & Fattah, M. A. (2020). Efficiency of the SPAW model in estimation of saturated hydraulic conductivity in calcareous soils. Journal of University of Duhok, 23(2), 189–201. https://journal.uod.ac/index.php/uodjournal/article/view/872/621

Kotlar, A. M., Jong van Lier, Q., Barros, A. H. C., Iversen, B. v., & Vereecken, H. (2019). Development and Uncertainty Assessment of Pedotransfer Functions for Predicting Water Contents at Specific Pressure Heads. Vadose Zone Journal, 18(1), 190063. https://doi.org/10.2136/vzj2019.06.0063

Legates, D. R., & Mccabe, G. J. (1999). Evaluating the use of "goodness-of-fit" Measures in hydrologic and hydroclimatic model validation. Water Resources

Research, 35(1), 233–241. https://doi.org/10.1029/1998WR900018

Li, Y., Chen, D., White, R. E., Zhu, A., & Zhang, J. (2007). Estimating soil hydraulic properties of Fengqiu County soils in the North China Plain using pedo-transfer functions. In Geoderma (Vol. 138, Issues 3–4). https://doi.org/10.1016/j.geoderma.2006.11.018

Longley, P. A., & Frank Goodchild, M. (2020). Geographic Information Science and Systems. In International Encyclopedia of Human Geography. https://doi.org/10.1016/b978-0-08-102295-5.10557-8

McCuen, R. H., Knight, Z., & Cutter, A. G. (2006). Evaluation of the Nash–Sutcliffe Efficiency Index. Journal of Hydrologic Engineering, 11(6), 597–602. https://doi.org/10.1061/(ASCE)1084-0699(2006)11:6(597)

Moriasi, D. N., Arnold, J. G., M. W. Van Liew, R. L. Bingner, R. D. Harmel, T. L. Veith, van Liew, M. W., Bingner, R. L., Harmel R. D., Veith T.L., M. W. Van Liew, R. L. Bingner, R. D. Harmel, & T. L. Veith. (2007). Model Evaluation Guidelines for Systematic Quantification of Accuracy in Watershed Simulations. Transactions of the ASABE, 50(3), 885–900. https://doi.org/10.13031/2013.23153

Moriasi, D. N., Gitau, M. W., Pai, N., & Daggupati, P. (2015). Hydrologic and water quality models: Performance measures and evaluation criteria. Transactions of the ASABE, 58(6), 1763–1785. https://doi.org/10.13031/trans.58.10715

Nash, J. E., & Sutcliffe, J. V. (1970). River flow forecasting through conceptual models part I — A discussion of principles. Journal of Hydrology, 10(3), 282–290.https://doi.org/10.1016/0022-694(70)90255-6

Omran, W., Abd El-Mageed, T., Sweed, A., & Awad, A. (2022). A modified equation for fitting the shape feature of the entire soil water characteristic curves. Egyptian Journal of Soil Science, 63(1), 15–34. https://doi.org/10.21608/ejss.2022.164765.1541

Ostovari, Y., Asgari, K., & Cornelis, W. (2015). Performance Evaluation of Pedotransfer Functions to Predict Field Capacity and Permanent Wilting Point Using UNSODA and HYPRES Datasets. Arid Land Research and Management, 29(4), 383–398. https://doi.org/10.1080/15324982.2015.1029649

Ottoni, M. V., Ottoni Filho, T. B., Lopes-Assad, M. L. R. C., & Rotunno Filho, O. C. (2019). Pedotransfer functions for saturated hydraulic conductivity using a database with temperate and tropical climate soils. Journal of Hydrology, 575, 1345–1358. https://doi.org/10.1016/j.jhydrol.2019.05.050

Pachepsky, Y. A., Rajkai, K., & Tóth, B. (2015). Pedotransfer in soil physics: Trends and outlook - A review. Agrokemia Es Talajtan, 64(2), 339–360. https://doi.org/10.1556/0088.2015.64.2.3

Patil, N. G., Planning, L. U., & Singh, S. K. (2016). Pedotransfer Functions for Estimating Soil Hydraulic Properties : A Review Pedotransfer Functions for Estimating Soil Hydraulic Properties : A Review. 0160(December 2017). https://doi.org/10.1016/S1002-0160(15)60054-6

Perera, Y. Y., Zapata, C. E., Houston, W. N., & Houston, S. L. (2005). Prediction of the Soil-Water Characteristic Curve Based on Grain-Size-Distribution and Index Properties. 40776(August), 1–12. https://doi.org/10.1061/40776(155)4

Rafie, R. M., & El-Boraie, F. M. (2017). Effect of Drip Irrigation System on Moisture and Salt Distribution Patterns under North Sinai Conditions. *Egyptian Journal of Soil Science*, *57*(3), 247–260. https://doi.org/10.21608/ejss.2017.4158

Reynolds, W. D., Elrick, D. E., Youngs, E. G., Booltink, H. W. G., & Bouma, J. (2002). Methods of Soil Analysis: Part 4 Physical Methods (J. H. Dane & G. Clarke Topp, Eds.). Soil Science Society of America. https://doi.org/10.2136/sssabookser5.4

Rowell, D. L. (1994). Soil Science : Methods & Applications. In Soil Science.

Santra, P., Kumar, M., Kumawat, R. N., Painuli, D. K., Hati, K. M., Heuvelink, G. B. M., & Batjes, N. H. (2018). Pedotransfer functions to estimate soil water content at field capacity and permanent wilting point in hot Arid Western India. Journal of Earth System Science, 127(3), 35. https://doi.org/10.1007/s12040-018-0937-0

Saxton, K. E., Rawls, W. J., Romberger, J. S., & Papendick, R. I. (1986). Estimating Generalized Soil-water Characteristics from Texture. Soil Science Society of America Journal, 50(4), NP-NP. https://doi.org/10.2136/sssaj1986.03615995005000040054x

Schaap, M. G. (2004). Accuracy and uncertainty in PTF predictions. In and W. J. R. Y. Pachepsky (Ed.), Developments in Soil Science, Development of Pedotransfer Functions in Soil Hydrology (Vol. 30, Issue C, pp. 33–43). Elsevier B.V. https://doi.org/10.1016/S0166-2481(04)30003-6

Schaap, M. G., Leij, F. J., & van Genuchten, M. Th. (1998). Neural Network Analysis for Hierarchical Prediction of Soil Hydraulic Properties. Soil Science Society of America Journal, 62(4), 847–855. http://doi.wiley.com/10.2136/sssaj1940.036159950004000C0132x

Shiri, J., Keshavarzi, A., Kisi, O., & Karimi, S. (2017). Using soil easily measured parameters for estimating soil water capacity: Soft computing approaches. Computers and Electronics in Agriculture, 141, 327–339. https://doi.org/10.1016/j.compag.2017.08.012

Shwetha, P., & Prasanna, K. (2018). Pedotransfer Functions for the Estimation of Saturated Hydraulic Conductivity for Some Indian Sandy Soils 1. 51(9), 1042–1049. https://doi.org/10.1134/S1064229318090119

Sobieraj, J. A., Elsenbeer, H., & Cameron, G. (2004). Scale dependency in spatial patterns of saturated hydraulic conductivity. CATENA, 55(1), 49–77. https://doi.org/10.1016/S0341-8162(03)00090-0

Sun, H., Lee, J., Chen, X., & Zhuang, J. (2020). Estimating soil water retention for wide ranges of pressure head and bulk density based on a fractional bulk density concept. Scientific Reports, 10(16666), 1–12. https://doi.org/10.1038/s41598-020-73890-8

Tomasella, J., Hodnett, M. G., & Rossato, L. (2000). Pedotransfer Functions for the Estimation of Soil Water Retention in Brazilian Soils. Soil Science Society of America Journal, 64(1), 327–338. https://doi.org/10.2136/sssaj2000.641327x

Tomasella, J., & Pachepsky, Y. (2003). Comparison of Two Techniques to Develop Pedotransfer Functions for Water Retention. May 2014. https://doi.org/10.2136/sssaj2003.1085.

Trejo-Alonso, J., Fuentes, C., Chávez, C., Quevedo, A., Gutierrez-Lopez, A., & González-Correa, B. (2021). Saturated hydraulic conductivity estimation using artificial neural networks. Water (Switzerland), 13(5), 1–15. https://doi.org/10.3390/w13050705

Twarakavi, N. K. C., Šimůnek, J., & Schaap, M. G. (2009). Development of Pedotransfer Functions for Estimation of Soil Hydraulic Parameters using Support Vector Machines. Soil Science Society of America Journal, 73(5), 1443–1452. https://doi.org/10.2136/sssaj2008.0021

Ungaro, F., Calzolari, C., & Busoni, E. (2005). Development of pedotransfer functions using a group method of data handling for the soil of the Pianura Padano–Veneta region of North Italy: water retention properties. Geoderma, 124(3–4), 293–317. https://doi.org/10.1016/j.geoderma.2004.05.007

Vereecken, H., Diels, J., van Orshoven, J., Feyen, J., & Bouma, J. (1992). Functional Evaluation of Pedotransfer Functions for the Estimation of Soil Hydraulic Properties. Soil Science Society of America Journal, 56(5), 1371–1378. https://doi.org/10.2136/sssaj1992.03615995005600050007x

Weynants, M., Vereecken, H., & Javaux, M. (2009). Revisiting Vereecken Pedotransfer Functions: Introducing a Closed-Form Hydraulic Model. Vadose Zone Journal, 8(1), 86–95. https://doi.org/10.2136/vzj2008.0062

Wilcox, B. P., Rawls, W. J., Brakensiek, D. L., & Wight, J. R. (1990). Predicting runoff from Rangeland Catchments: A comparison of two models. Water Resources Research, 26(10), 2401–2410. https://doi.org/10.1029/WR026i010p02401

Wösten, J. H. M., Finke, P. A., & Jansen, M. J. W. (1995). Comparison of class and continuous pedotransfer functions to generate soil hydraulic characteristics. Geoderma, 66(3–4), 227–237. https://doi.org/10.1016/0016-7061(94)00079-P

Zapata, C. E., Houston, W. N., Houston, S. L., & Walsh, K. D. (2000). Soil-water characteristic curve variability. Proceedings of Sessions of Geo-Denver 2000 - Advances in Unsaturated Geotechnics, GSP 99, 287(July), 84–124. https://doi.org/10.1061/40510(287)7

Zhang, X., Zhu, J., Wendroth, O., Matocha, C., & Edwards, D. (2019). Effect of Macroporosity on Pedotransfer Function Estimates at the Field Scale. Vadose Zone Journal, 18(1), 1–15. https://doi.org/10.2136/vzj2018.08.0151

Zhang, Y., & Schaap, M. G. (2019). Estimation of saturated hydraulic conductivity with pedotransfer functions: A review. Journal of Hydrology, 575(June), 1011–1030. https://doi.org/10.1016/j.jhydrol.2019.05.058

Zhao, C., Shao, M., Jia, X., Nasir, M., & Zhang, C. (2016). Using pedotransfer functions to estimate soil hydraulic conductivity in the Loess Plateau of China. Catena, 143, 1–6. https://doi.org/10.1016/j.catena.2016.03.037.